*Optica Applicata, Vol. XLII, No. 3, 2012*
DOI: 10.5277/oa120313

# Study of the pump absorption efficiency in D-shaped double clad optical fiber

ROBERTO NARRO-GARCÍA*, MIGUEL ARRONTE, JESUS GUERRERO-CONTRERAS, EUGENIO RODRÍGUEZ

Laboratorio de Tecnología Láser, CICATA-IPN Unidad Altamira,
km 14.5 Carr. Tampico-Puerto Ind. Altamira, Altamira 89600, TAMPS, México

*Corresponding author: rnarro@ipn.mx

In this paper, we evaluate numerically the pump absorption efficiency in a D-shaped fiber. The study is carried out through the ray tracing method in three dimensions. The simulation results show that D-shaped fiber has higher pump power absorption when the core is place off the geometric center of the inner cladding. On the other hand, when the incidence of the pump beam is off the geometrical center of the fiber cross-section or the angle of incidence increases, the pump absorption efficiency decreases in a circular-shaped fiber, while in D-shaped fiber it is higher and is kept constant.

Keywords: pump absorption efficiency, D-shaped fiber, double clad fibers.

## 1. Introduction

Power scaling in conventional single clad rare earth doped monomode fibers is limited because of the incompatibility of these fibers with the beam-quality of high power diode laser arrays. Therefore, special double clad fiber designs have been developed. In double clad fibers the pump light is coupled from the inner clad into the active core over the entire fiber length [1–3]. Previous reports show that a greater efficiency of the pumping absorption in double clad optical fibers can be achieved by varying the geometry of the inner clad. For example, LIU and UEDA [4] demonstrated that the efficiency of pumping absorption in double clad fibers with off-center core or rectangular inner clad can be up to four times greater than the efficiency of the pumping absorption in fibers with circular inner clad and core in the geometric center of the fiber. To date, there are a variety of cladding geometries to improve pump absorption, *e.g.*, circular offset, rectangular, D-shaped, hexagonal, 2-truncation circle, *etc*. [5–8].

D-shaped fiber has been widely used in high-power double-clad fiber lasers because of its high pump absorption efficiency. In these fibers, the propagation of the pump light becomes chaotic. Hence, every launched ray of the pump light will cross the active core of the fiber and thus be absorbed. The D-shaped fiber in addition has the advantage of its shape being almost round so that it can be cleaved and handled easily, and it can be polished into standard fiber connectors [9]. Recently, GORJAN *et al*. [10] performed measurements of pump absorption via fluorescence in a commercial D-shaped and circular fiber, obtaining experimentally 99% and 80% efficiency of the pumping absorption, respectively.

In this paper, we evaluate numerically the pump absorption efficiency in a D-shaped fiber. The pump absorption efficiency is evaluated depending on: *i*) the geometry of the inner clad, *ii*) the incidence position of the pump beam, and *iii*) the incidence angle of the pump beam on the initial fiber face. The study is carried out through the ray tracing method in three dimensions. The simulation results show the geometry of the inner clad and the core position in the D-shaped fiber that maximize the pump power absorption. On the other hand, a comparison of the pump absorption efficiency of a circular-shaped and D-shaped fiber is reported. When the incidence of the pump beam is off the geometrical center of the fiber cross-section, or the incidence angle increases, the pump absorption efficiency decreases in a circular-shaped fiber, while in D-shaped fiber remains constant.

## 2. Description of the experiment

In this paper, we evaluate the propagation of a large number of rays through a circular and a D-shaped double clad fiber. The beam paths are evaluated in 3 dimensions using a ray tracing algorithm. This algorithm is based on the decomposition of the fiber into small triangular planes, which simplifies the problem of finding the intersection of the beam with each object in the fiber. In all the cases, a Gaussian beam of 980 nm wavelength with 0.1 rad of acceptance cone was coupled to the inner clad at the entrance face of the fiber. The parameters of the fibers analyzed were assumed as for commercially available silica fibers: a numerical aperture of the core/clad equals 0.12/0.499; and an absorption coefficient of the core/clad $\alpha = 64.5\ \mathrm{m^{-1}}/6.91\times10^{-4}\ \mathrm{m^{-1}}$.

In Section 3.1, the intensity profile variations depending on the D-shape inner clad are studied. Figure 1 shows the cross-section of the D-shaped inner clad under study. In this section, the intensity profiles are evaluated for two fibers with diameters of 300 μm and 350 μm, respectively. In each case the asymmetrical parameter $e = d - D$ was varied within the interval $d/2 \le e \le d$, using 10 μm steps. Each ray being evaluated

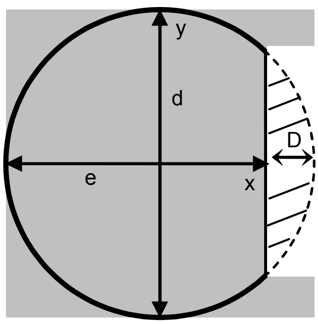


Fig. 1. Schematic representation of the D-shaped geometry; $d$ is the inner clad diameter and $e = d - D$ is the asymmetrical parameter.

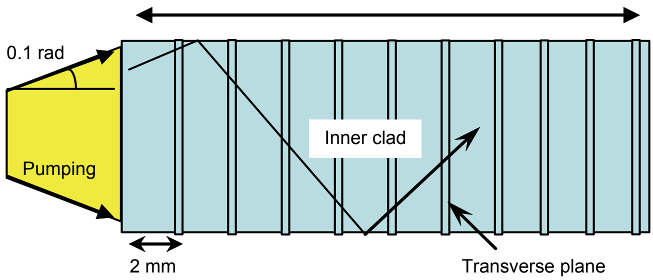


Fig. 2. Lateral representation of the pump beam coupling to the fiber and distribution of the transverse planes.

is transmitted along the fiber undergoing multiple internal reflections on the walls of the inner clad until it finally reaches the exit face of the fiber. During the simulations of the path for each ray, whenever it intersects a plane transverse to the fiber length, both the ray intensity and the coordinates of the intersection point are calculated and stored. The program evaluates the intensity profile for a total of 10 different transverse planes, parallel to each other and spaced at 2 mm, as schematically depicted in Fig. 2. Each of these fiber transverse planes was discretized into $10 \times 10$ $\mu m^2$ sections. Finally, the results obtained for each one of these planes are superposed (added) giving rise to the values of the total intensity of radiation crossing each of the fiber sectors.

The algorithm described in Sections 3.2 and 3.3 takes into account the losses by reflexion (at the clad and core boundaries) and absorption (by the core). Each time a ray passes from one medium to another the amount of reflexion is calculated by means of the Fresnel coefficients. On the other hand, each time the ray passes through a fiber object (core or inner clad) the amount of radiation absorbed by that object is calculated according to the expression:

$$\frac{I_{out}}{I_{in}} = e^{-\alpha x} \tag{1}$$

where $I_{in}$ is the intensity at the entry of the object, $x$ is the distance traveled by the beam within the object, and $\alpha$ is the absorption coefficient. In these sections the total radiation $I_T$ is defined as the sum of the radiation of each ray:

$$I_T = \sum_{i=1}^{N} I_i \tag{2}$$

where $N$ is the number of rays that are evaluated and $I_i$ is radiation intensity of each ray defined as:

$$I_i = I_{i1} + I_{i2} + I_{i3} + I_{i4} \tag{3}$$

where: $I_{i1}$ is the radiation that is reflected from the entrance face of the fiber; $I_{i2}$ is the radiation that is refracted from the inner clad to the external clad; $I_{i3}$ is the radiation

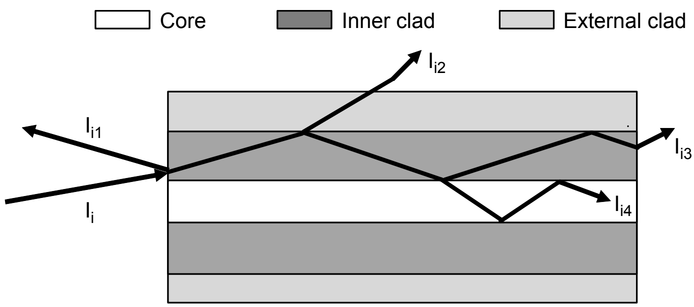


Fig. 3. Representation of the trajectory of a ray inside a double clad fiber.

that was not absorbed within the fiber and therefore reaches the exit face of the fiber, and $I_{i4}$ is the radiation that was absorbed by the core (Fig. 3).

In Section 3.2, a study is conducted in order to compare the absorption between a circular- and a D-shaped fiber depending on the pump launching point on the fiber cross-section. In both cases, the fibers are 4 m long and the core is located at the geometric center of the fiber. The geometric characteristics of each fiber are presented in Table 1.

T a b l e 1. Optical and geometric characteristics of the DCFs during the simulations.

| Fiber code | Shape | *e* | Core diameter [μm] | Clad diameter [μm] |
|---|---|---|---|---|
| 30/300/CC | Circular | 300 | 30 | 300 |
| 30/350/D | D-shaped | 293 | 20 | 350 |

The position of the pump beam center was varied within the interval $0 \le T \le r/2$ using 15 μm steps, thus operating a transverse offset $T$, and consequently launching the beam into the inner clad as schematically depicted in Fig. 4. To simplify the calculations, the position of the pump beam incidence was varied only along

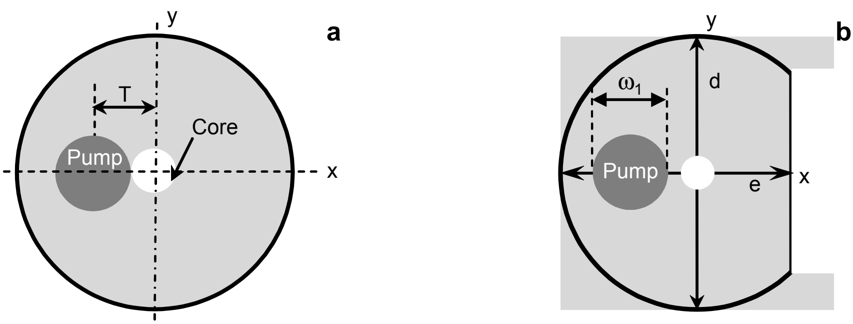


Fig. 4. Cross-section of the fiber entrance face for the two fibers compared in this section. The geometrical dimensions are presented in Table 1. Fiber code 30/300/CC (**a**) and fiber code 30/350/D (**b**). In both cases, the pump beam center is displaced along the *x*-axis the distance $T$ from the geometrical center of the fiber, thus operating a transverse offset, and consequently launching the pump beam into the inner clad.

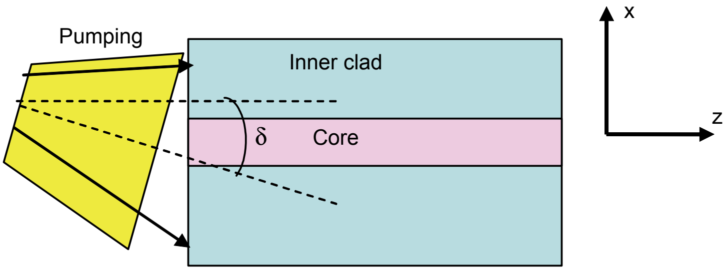


Fig. 5. Lateral representation of the pump beam coupling to the double clad fiber.

the $x$-axis. The diameter of the pump beam $\omega_1$ was 70 μm for all the calculations, to ensure that in each simulation the beam is fully contained within the fiber inner clad.

For each one of the test fibers it was studied how the transverse offset of the pump beam influences both the pump absorption efficiency (4) and the amount of radiation reaching the exit face of the fiber (5)

$$E_{abs} = \frac{\sum_{i=1}^{N} I_{i4}}{I_T} \tag{4}$$

$$E_{out} = \frac{\sum_{i=1}^{N} I_{i3}}{I_T} \tag{5}$$

In Section 3.3, the $E_{abs}$ and $E_{out}$ between a circular and a D-shaped fiber (30/300/CC and 30/350/D) depending on the incidence angle $\delta$ of the pump beam are studied. Similarly to the experiments conducted in the previous paragraph, $E_{abs}$ and $E_{out}$ are calculated as a function of the incidence angle $\delta$ of the pump beam. The diameter of the pump beam $\omega_1$ was 100 μm. The angle $\delta$ is measured in relation to the surface normal, as schematically presented in Fig. 5. Considering that the numerical aperture of the inner clad is 0.499, the incidence angle or acceptance cone should be lower than 0.52 rad (29.8°), consequently during the calculations $\delta$ was varied within the interval 0.05 rad $< \delta <$ 0.3 rad.

## 3. Results and discussion

### 3.1. Intensity profile variations depending on the parameter *e* for a D-shaped inner clad without core

In Figure 6, two typical examples are presented of the calculated intensity profiles for two different values of the asymmetrical parameter *e*. In these calculations, neither the presence of the core nor the inner clad absorption were considered.

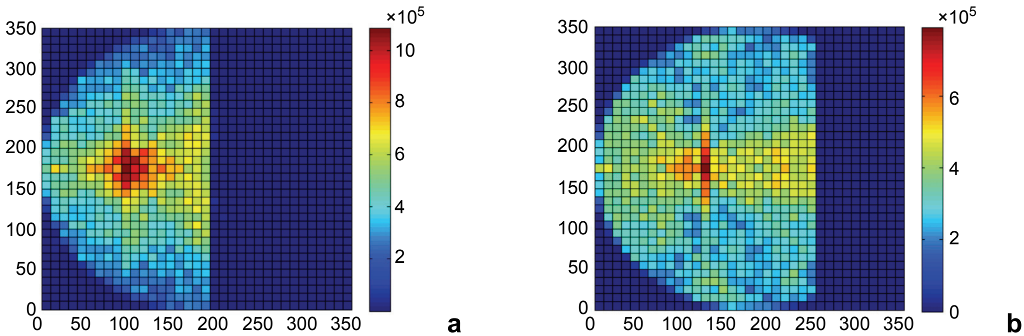


Fig. 6. Cumulative intensity profile in a D-shaped inner clad for two different configurations: (**a**) clad with $d = 350$ μm and $e = 190$ μm. The maximum intensity was obtained at profile position $(x, y) = (95, 175)$, *i.e.*, at a distance $s = 80$ μm off the clad center. (**b**) Clad with $d = 350$ μm and $e = 250$ μm. The maximum intensity was obtained at position $(x, y) = (125, 175)$ of the profile, *i.e.*, at a distance $s = 50$ μm off the clad center. Each 10×10 μm$^2$ section is assigned a color ranging from dark blue (lowest intensity) to dark red (highest intensity).

Both images reveal that the area with the largest intensity is displaced from the geometric center of the clad a certain distance $s$. Examples depicted in Fig. 6 yield the value $s = 80$ μm for profile ($d = 350$ μm, $e = 190$ μm) and $s = 50$ μm for profile ($d = 350$ μm, $e = 250$ μm).

The intensity value accumulated in each sector is a measure of the number of rays crossing this area unit, consequently the area exhibiting the largest intensity represents the region of the clad cross-section through which the highest number of rays propagates. In this sense, the intensity of radiation passing through a particular area

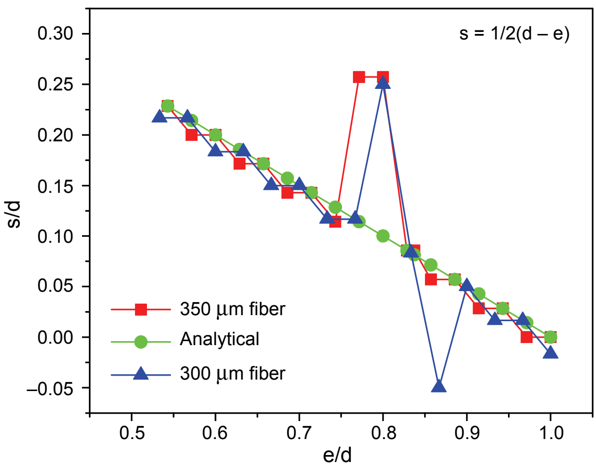


Fig. 7. Relationship between the position of maximum intensity $s$ (measured from geometric center of the clad) and the asymmetrical parameter $e$ for two D-shaped fibers. The analytical calculation by Eq. (6) was included for comparison.

of the clad cross-section is a measure of the pump absorption efficiency. In order to find out the optimal position where to place the fiber core, the following analysis was performed: the position $s$ for the maximum intensity section was plotted as a function of the asymmetrical parameter $e$ for the two fibers studied. For comparison purposes, both the $s$ and $e$ values were normalized to the diameter $d$ of each fiber. The results of this analysis are shown in Fig. 7.

With the exception of the $s$ values obtained for the interval $0.75 < e/d < 0.85$, all other values fit well a linear dependence $s = f(e)$. The relationship obtained by linear regression to experimental data was:

$$s = \frac{1}{2}(d - e) \tag{6}$$

As mentioned above, several calculations were performed to study the influence of asymmetry parameter $e$ on the intensity distribution over the clad cross-section. A total of 18 and 15 profiles were calculated for fibers with 350 μm and 300 μm diameter, respectively. To find out the optimum value of the parameter $e$ for an efficient pumping of the fiber core the following analysis was carried out: the maximum intensity value obtained for each intensity profile was plotted as a function of the ratio $e/d$ for the two fibers considered in the present work. The intensity maxima were normalized to the highest intensity value found among all calculated profiles. The results of this analysis are presented in Fig. 8.

As can be observed, the normalized intensities for both fiber geometries exhibit maxima when the ratio $e/d$ approaches 0.5 and 1.0, respectively. For these values we would expect efficient pumping absorption. The curves also show a minimum region within the interval $0.75 < e/d < 0.85$, indicating that a geometry with these dimensions

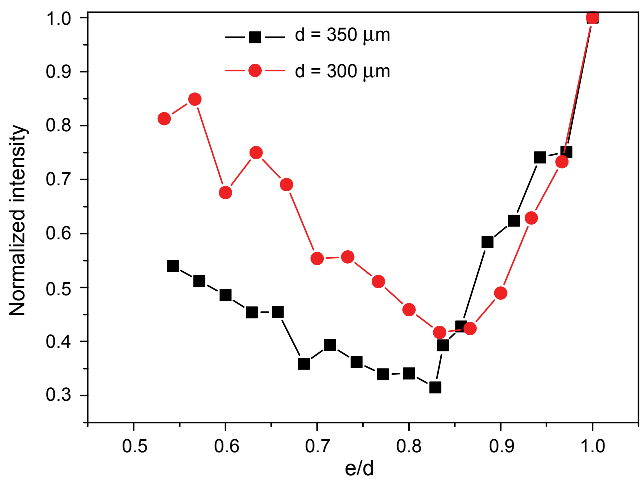


Fig. 8. Normalized intensity vs. ratio $e/d$ for all calculated fiber geometries. Calculations were performed for two D-shaped fibers with diameters of the inner clad of 300 μm and 350 μm, respectively. The intensity maxima were normalized to the highest value found in all the profiles calculated.

should be inefficient (the commercial fiber studied has a ratio *e*/*d* in this range). The fact that configurations with *e*/*d* ratio within the above-mentioned interval are inefficient could be the reason for the deviation from the linear behavior the function $s = f(e)$ exhibits in this interval.

### 3.2. Dependence of absorption efficiency on the position where the pump beam is launched on the fiber cross-section

The results of these simulations are presented in Fig. 9. For fiber 30/300/CC, the results exhibit a decrease in the core absorption by increasing the transverse offset *T*, *i.e.*, when the pump beam is shifted away from the geometric center of the fiber. Under these conditions the number of helical rays increases, *i.e.*, those which travel primarily through the clad and therefore are not absorbed in the core. Because of the low absorption the helical rays undergo inside the core, a considerable amount of pump light gets to reach the exit face of the fiber, increasing the value of $E_{out}$.

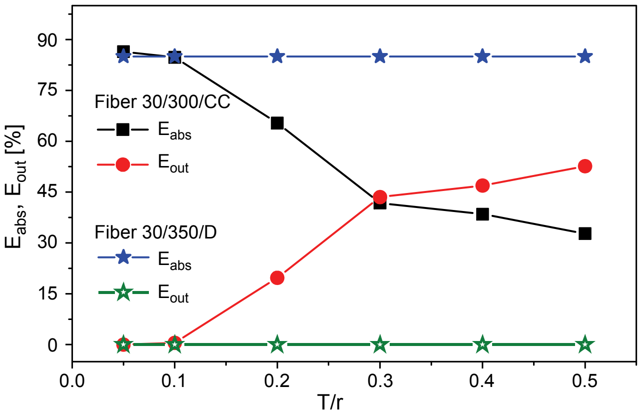


Fig. 9. Simulated results for the absorbed and transmitted signal vs. transverse offset *T* in double clad fibers 30/300/CC and 30/350/D.

For fiber 30/350/D both the $E_{abs}$ and $E_{out}$ remain constant independent of the transverse offset. This is because the geometry of type D breaks the helical modes, forcing the rays to pass through the center of the circle at some point of its travel, thus promoting the fact that they are absorbed by the core.

### 3.3. Study of the absorption efficiency depending on the incidence angle of the pump beam

The results for $E_{abs}$ and $E_{out}$ are presented in Fig. 10. Fiber 30/300/CC exhibits a similar behavior to that described in the previous section. By increasing the pump incidence angle up to 0.15 rad (8.5°), the $E_{abs}$ decreases and the $E_{out}$ increases. These results are consistent with an increase in the number of helical rays by increasing the incidence angle $\delta$. The periodic trajectories of these rays can exhibit poor overlap with the fiber

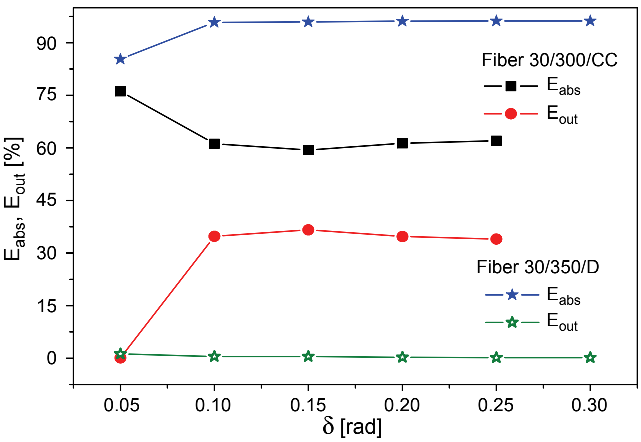


Fig. 10. Simulated results of $E_{abs}$ and $E_{out}$ vs. the incidence angle $\delta$ in double clad fibers 30/300/CC and 30/350/D.

core and therefore the absorption efficiency will tend to decrease. The lower the amount of the pump light not absorbed inside the fiber core, the higher the amount or radiation reaching the exit fiber face.

Fiber 30/350/D also exhibits a similar behavior to that described in the previous section. The $E_{out}$ is almost zero (below 0.5%) for all the interval studied 0.05 rad < $\delta$ < 0.3 rad. The value 1.2% presented for $\delta \approx 0.05$ rad, could be associated with the inhomogeneous rays distribution inside the inner clad at such small incidence angles.

## 4. Conclusions

In this paper, the pump absorption efficiency of D-shaped fibers of different geometries has been analyzed through the ray tracing method in three dimensions. The D-shaped fibers were analyzed using two different pumping schemes and the results of the simulations were compared with a commercial circular-shaped fiber.

In the case where the pumping is perfectly perpendicular to the entrance face of the D-shaped fiber and is focused just in the geometrical center, an analytical expression was determined that can predict the best position of the core. This expression indicates that the best position of the core is off the geometrical center of the fiber cross-section. It was shown that under this optimal pumping condition, the pump absorption efficiency can be maximized when the ratio *e*/*d* approaches the values of 0.5 and 1.0, respectively.

On the other hand, when the incidence of the pump beam (where the pump beam is launched on the fiber cross-section) is off the geometrical center of the fiber cross-section or when the angle of incidence $\delta > 0.10$ rad, the pump absorption efficiency decreases in a circular-shaped fiber while in D-shaped fiber the pump absorption efficiency is higher and it is kept constant. Table 2 summarizes

Table 2. Results of the pump absorption efficiency for two different pumping schemes.

| | Pump absorption efficiency $E_{abs}$ | | |
|---|---|---|---|
| | Gorjan *et al.* [10] | As a function of $T$ | As a function of $\delta$ |
| Circular-shaped | 80% | 32–86% | 62–76% |
| D-shaped | 99% | 85% | 96% |

the simulation results of the pump absorption efficiency depending on $T$ and $\delta$. It is shown that the simulations results are in agreement with the experimental results of GORJAN *et al.* [10]. The authors would like to emphasize that the best advantages of using a D-shaped fiber is that it is less sensible to the pumping problems than the circular-shaped fibers.

*Acknowledgements* – The authors would like to thank the Mexican agencies CONACYT, FOMIX--COTACYT and COFAA for their financial support.

## References

[1] UEDA K., LIU A., *Future of high-power fiber lasers*, Laser Physics **8**, 1998, pp. 774–781.
[2] DOMINIC V., MACCORMACK S., WAARTS R., SANDERS S., BICKNESE S., DOHLE R., WOLAK E., YEH P.S., ZUKER E., *110 W fiber laser*, Electronics Letters **35**(14), 1999, pp. 1158–1160
[3] NAM SEONG KIM, TOSHIHIRO HAMADA, MAHENDRA PRABHU, CHENG LI, JIE SONG, KEN-ICHI UEDA, ANPING LIU, HONG JIN KONG, *Numerical analysis and experimental results of output performance for Nd-doped double-clad fiber lasers*, Optics Communications **180**(4–6), 2000, pp. 329–337.
[4] ANPING LIU, KENICHI UEDA, *The absorption characteristics of circular, offset, and rectangular double-clad fibers*, Optics Communications **132**(5–6), 1996, pp. 511–518.
[5] YAHUA LI, JACKSON S.D., FLEMING S., *High absorption and low splice loss properties of hexagonal double-clad fiber*, IEEE Photonics Technology Letters **16**(11), 2004, pp. 2502–2504.
[6] LIU A., SONG J., KAMATANI K., UEDA K., *Rectangular double-clad fibre laser with two end-bundled pump*, Electronics Letters **32**(18), 1996, pp. 1673–1674.
[7] GUIJIN XIA, JINGHAN DUAN, SHANGHONG ZHAO, SHUFU DONG, *Light propagation in the multi-mode double-clad erbium: ytterbium co-doped fiber: Theory and experiment*, Optics and Laser Technology **36**(4), 2004, pp. 273–277.
[8] LEPROUX P., FEVRIER S., DOYA V., ROY P., PAGNOUX D., *Modeling and optimization of double-clad fiber amplifiers using chaotic propagation of the pump*, Optical Fiber Technology **7**(4), 2001, pp. 324–329.
[9] ZELLMER H., TÜNNERMANN A., WELLING H., REICHEL V., *Double-clad fiber laser with 30 W output power*, [In] *Optical Amplifiers and Their Applications*, Optical Society America, Trends Optics and Photonics (OSA TOPs), Vol. 16, 1997, pp. 137–140, paper FAW18.
[10] GORJAN M., MARINČEK M., ČOPIČ M., *Pump absorption and temperature distribution in erbium--doped double-clad fluoride-glass fibers*, Optics Express **17**(22), 2009, pp. 19814–19822.

*Received September 9, 2011*
*in revised form January 11, 2012*